

Supporting Information

Fluorescence Quenching-Based Sensing of Ofloxacin Using Dual-Nuclear Terbium Complex

Lin-Bo Cao,^a Hao Wang,^a Tian-Tian Wang,^a Wen-Bin Sun^{*a}

^a Key Laboratory of Functional Inorganic Material Chemistry Ministry of Education, School of Chemistry and Material Science, Heilongjiang University, 74 Xuefu Road, Harbin 150080, P. R. China (E-mail: wenbinsun@126.com).

Materials and methods

All complexes were synthesized using readily available chemicals and solvents, without the need for further purification. Lanthanide compounds were synthesized under ambient temperature and pressure conditions. The infrared (IR) spectrum was recorded with the FTIR-650 spectrometer. Elemental analysis of the solid sample was conducted using the EURO EA3000. The melting point was measured with the XT-4 micro-melting point apparatus. Crystal data for complex **1** were obtained using an Xcalibur Eos Gemini diffractometer, employing Mo K α radiation ($\lambda = 0.71073 \text{ \AA}$). All data were recorded at a temperature of 293(2) K. The structure of **1** was solved using direct methods and refined on F^2 through full-matrix least-squares with the SHELXTL-2015 program and Olex2. All non-hydrogen atoms were refined using isomorphous displacement parameters. Crystallographic data for complex **1** are provided in Table S1 and Table S2. The crystal structure and phase composition of the samples were characterized by powder X-ray diffraction (PXRD, $\lambda = 0.154 \text{ nm}$) using Cu-K α radiation on a Rigaku Ultima IV X-ray diffractometer, with measurements taken between 5° and 50°.

Table S1 Crystallographic data for **1**

1	
Empirical formula	C ₃₀ H ₄₆ Cl ₄ N ₄ O ₁₂ Tb ₂
FW (g.mol ⁻¹)	1114.35
Crystal system	monoclinic
Space group	C2/c
Temperature (K)	293
<i>a</i> (Å)	19.6964(7)
<i>b</i> (Å)	17.1246(6)
<i>c</i> (Å)	12.4454(4)
α (°)	90
β (°)	89.952(3)
γ (°)	90
<i>V</i> (Å ³)	4197.7(2)
ρ_{cacl} (Mg.m ⁻³)	1.763
μ (mm ⁻¹)	3.655
<i>F</i> (000)	2192.0
Independent relections	3234
<i>R</i> _{int}	0.0266
<i>R</i> ₁ [$I > 2\sigma(I)$]	0.0249
<i>wR</i> ₂ (all data)	0.0567
Goodness of fit on <i>F</i> ²	1.046
CCDC number	2410015

Table S2 Selected bond lengths (\AA) and angles ($^\circ$) for **1**

Tb1-Tb1'	3.9382(4)	Tb1-Cl1	2.6803(11)
Tb1-O1	2.586(3)	Tb1-O2'	2.344(2)
Tb1-O2	2.324(3)	Tb1-O3	2.369(3)
Tb1-O5'	2.329(3)	Tb1-O4	2.664(3)
Tb1-Cl2	2.6333(11)	O2-C5	1.332(4)
Cl1-Tb1-Tb1'	94.35(3)	O1-Tb1-Cl1	143.70(7)
Cl2-Tb1-Tb1'	170.45(3)	O1-Tb1-C12	84.58(7)
Cl2-Tb1-Tb1'	93.26(4)	O1-Tb1-O5'	139.19(9)
Cl2-Tb1-Cl1	82.25(6)	O4-Tb1-Tb1'	84.53(8)
O2'-Tb1-Tb1	32.30(6)	O4-Tb1-Cl1	145.48(8)
O2-Tb1-Tb1	32.62(6)	O4-Tb1-Cl2	85.93(8)
O2'-Tb1-Cl1	79.73(7)	O4-Tb1-O2'	81.34(10)
O2-Tb1-Cl1	107.97(7)	O4-Tb1-O1	70.66(10)
O2-Tb1-Cl2	147.82(6)	O4-Tb1-O5'	70.00(10)
O2'-Tb1-Cl2	144.88(7)	O4-Tb1-O3	137.85(11)
O2-Tb1-O2'	64.92(10)	O5'-Tb1-Tb1'	94.06(6)
O2'-Tb1-O1	120.90(8)	O5'-Tb1-Cl1	75.69(7)
O2-Tb1-O1	63.92(8)	O3-Tb1-Tb1'	101.34(8)
O2-Tb1-O4	89.45(10)	O3-Tb1-Cl1	76.29(8)
O2'-Tb1-O5'	62.65(9)	O3-Tb1-Cl2	86.06(9)
O2-Tb1-O5'	125.70(9)	O3-Tb1-O1	67.41(10)
O2'-Tb1-O3	124.49(11)	O3-Tb1-O5'	148.86(10)
O2-Tb1-O3	76.23(10)	Tb1-O2-Tb1'	115.08(10)
O1-Tb1-Tb1'	92.65(6)	C5-O2-Tb1	122.7(2)

Table S3 Continuous Shape Measures (CShMs) of the coordination geometry in **1**. The three closer ideal geometries to the real complexes are listed and below are the symmetry and description for each polyhedron

Complex	<i>s</i>	Polyhedron		
1	2.732	BTPR-8	C_{2v}	Biaugmented trigonal prism
	3.083	JBTPR-8	C_{2v}	Biaugmented trigonal prism J50
	2.536	TDD-8	D_{2d}	Triangular dodecahedron

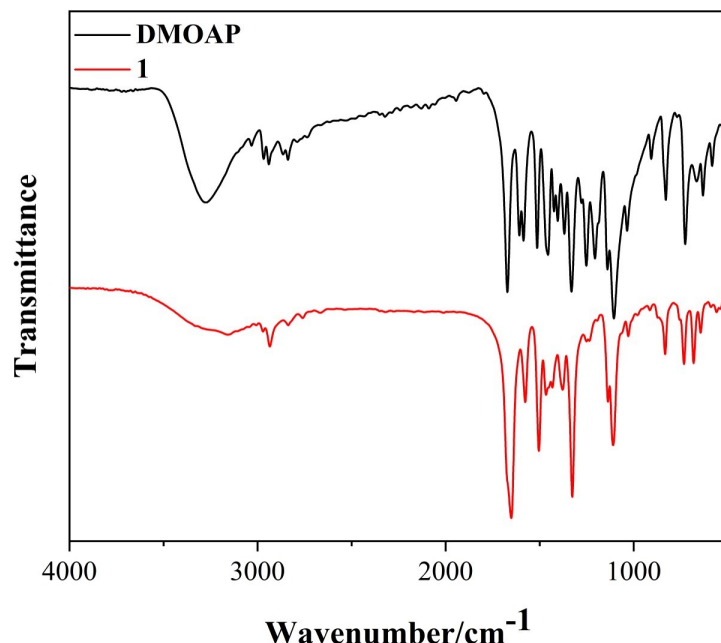


Fig. S1 IR spectrum of complex **1** and DMOAP.

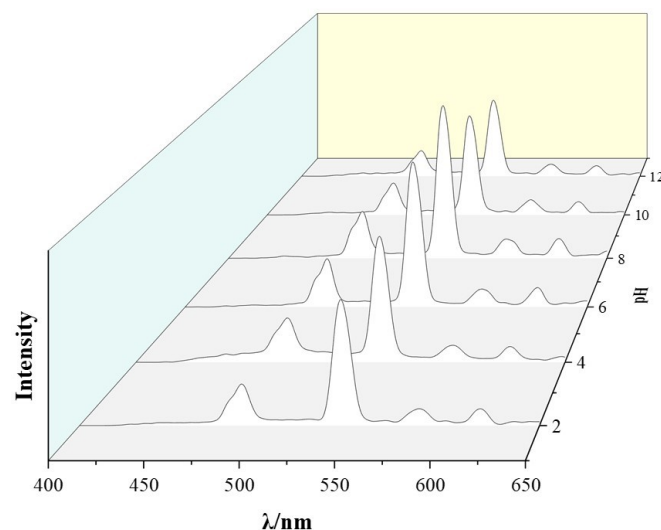


Fig. S2 luminescence intensity of filter powders at different pH values.



Fig. S3 Photograph of filter powders at various pH values.

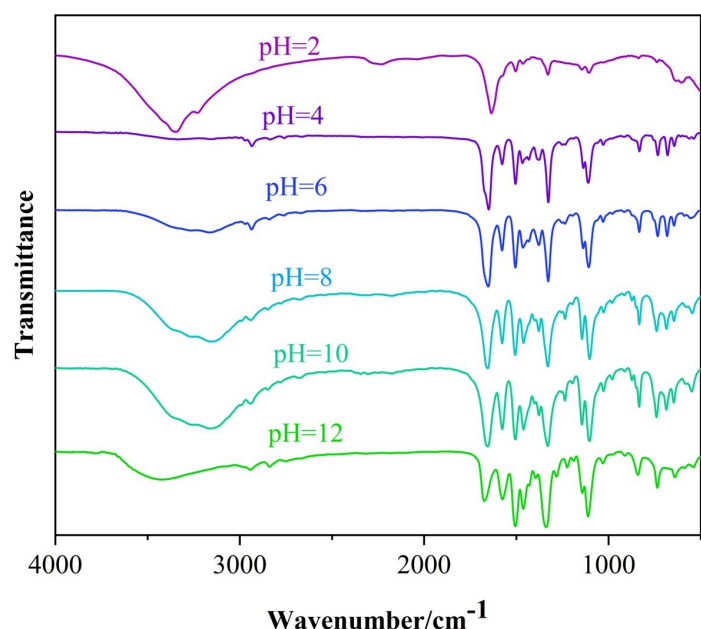


Fig. S4 IR spectrum of filter powders at different pH values.

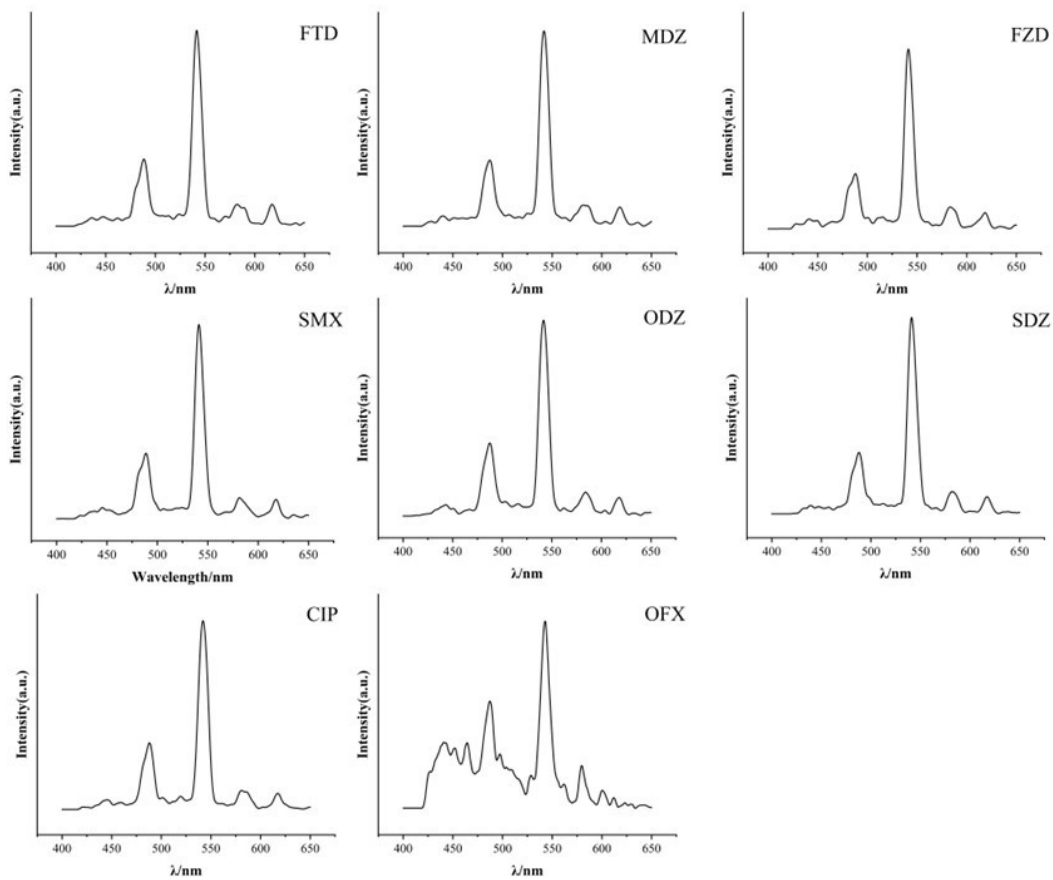


Fig. S5 The luminescence of complex **1** (1 mg/mL) in acetonitrile solution was corresponding to the interferences (1 mM) and OFX (1 mM).

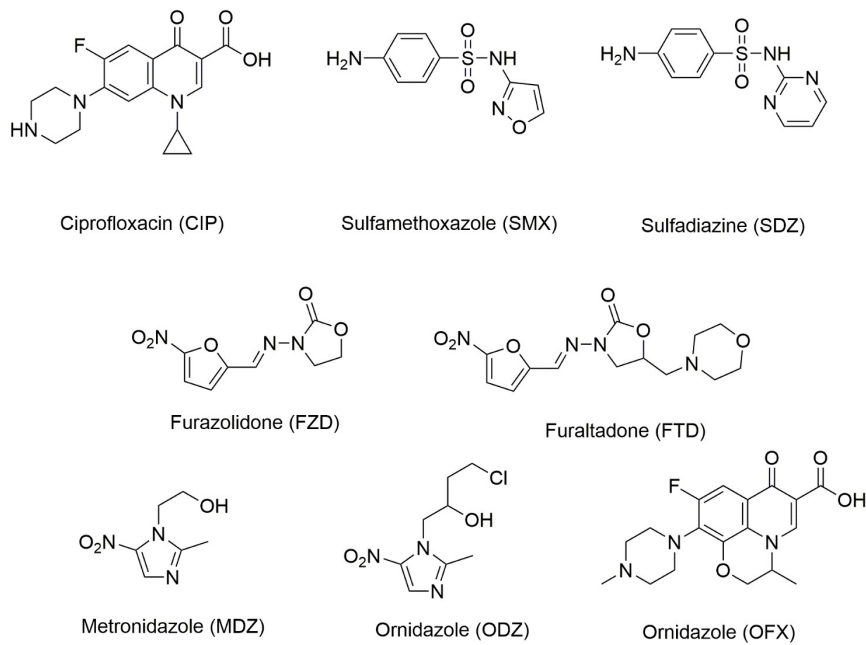


Fig. S6 Molecular structure of other antibiotics.

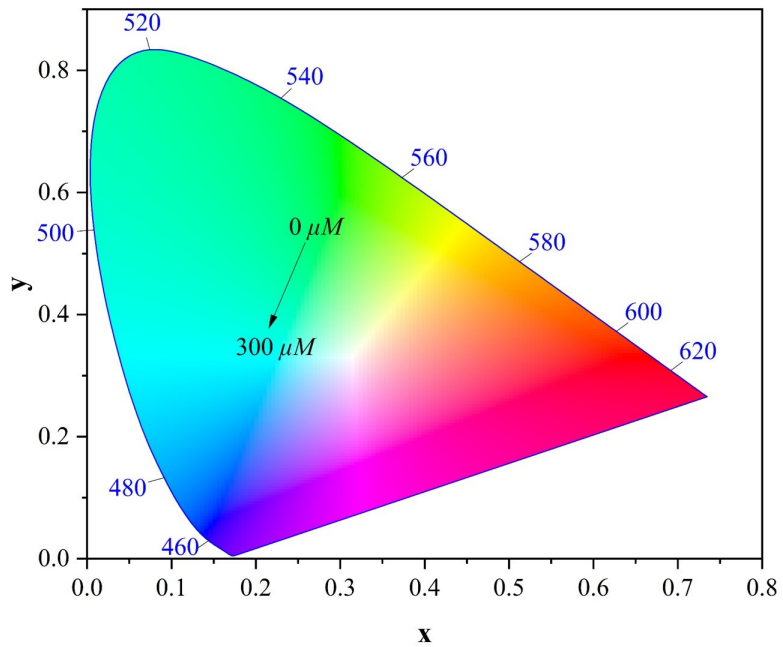


Fig. S7 CIE change values of complex **1** during the detection of OFX.

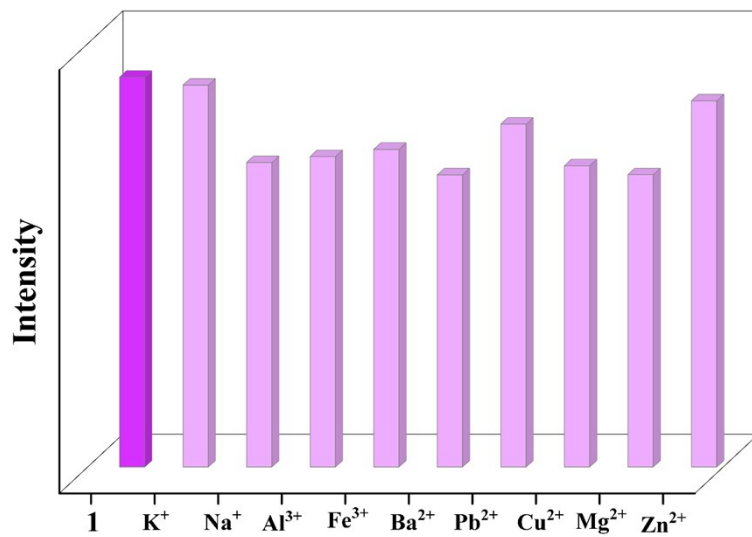


Fig. S8 Anti-interference detection of complex **1** (1 mg/mL) with various metal ions (1 mM).

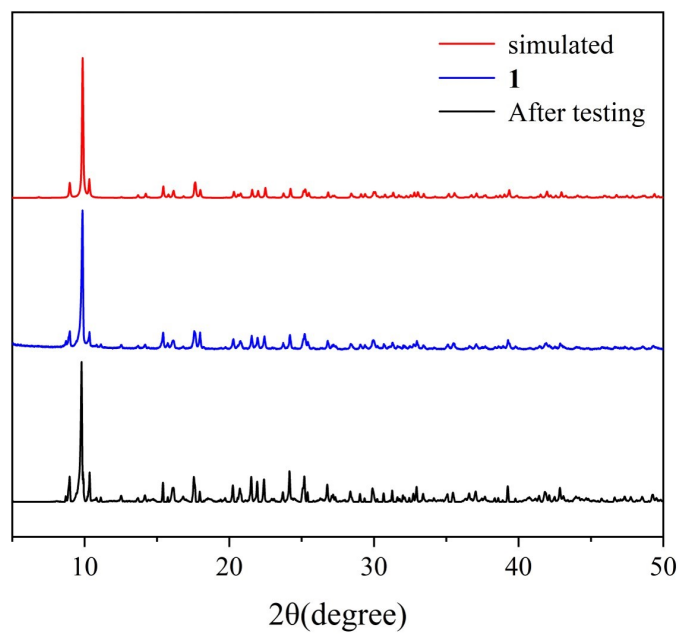


Fig. S9 PXRD spectrum of **1** and **1** after testing

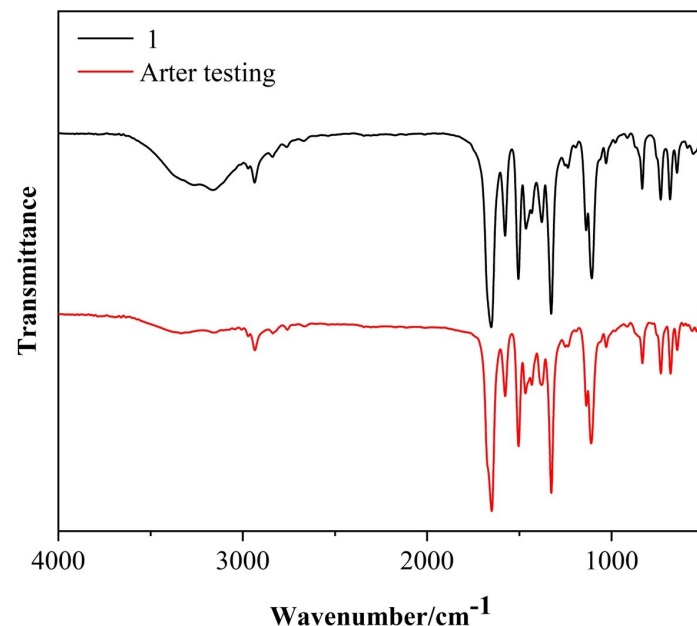


Fig. S10 IR spectrum of **1** and **1** after testing.

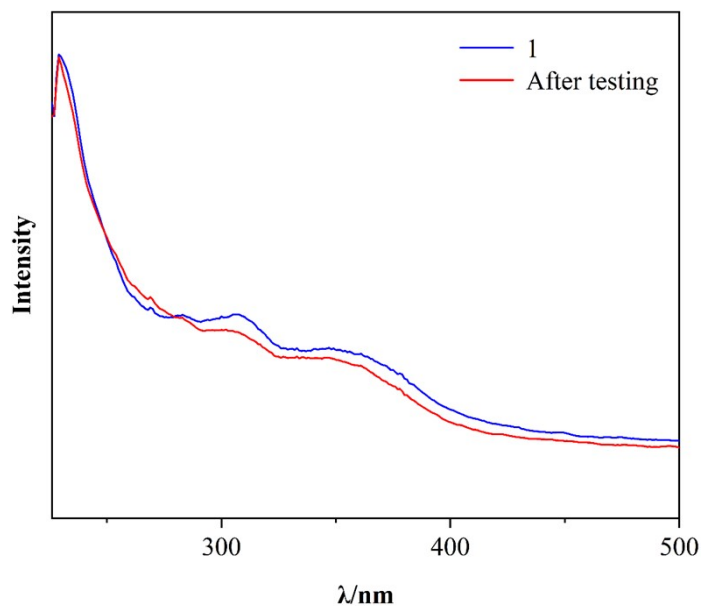


Fig. S11 UV-vis absorption spectra of **1** and **1**after testing in CH_3CN . ($c = 10^{-3} \text{ M}$, $\varepsilon = 3.5 \times 10^3 \text{ M}^{-1} \text{ cm}^{-1}$)

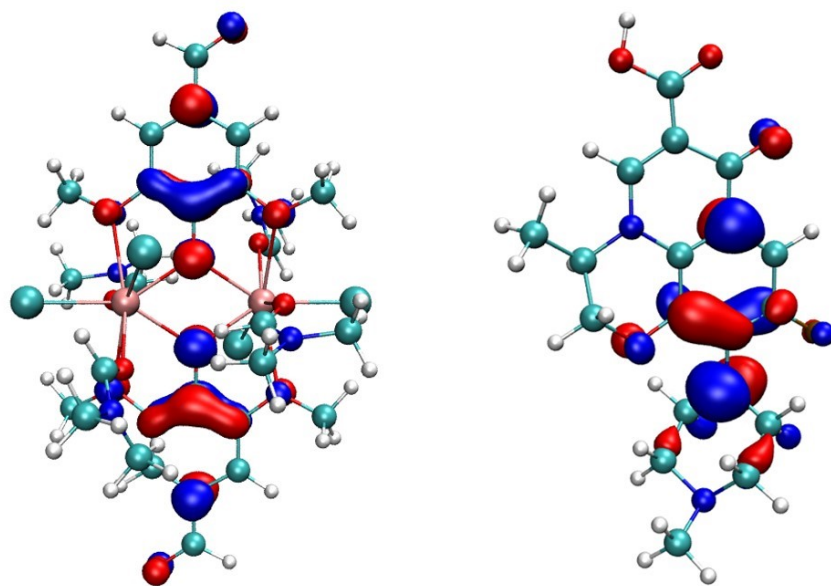


Fig. S12 HOMO electron densities of the ligand in **1** (left) and the free OFX (right) calculated by DFT (Gaussian16 package).

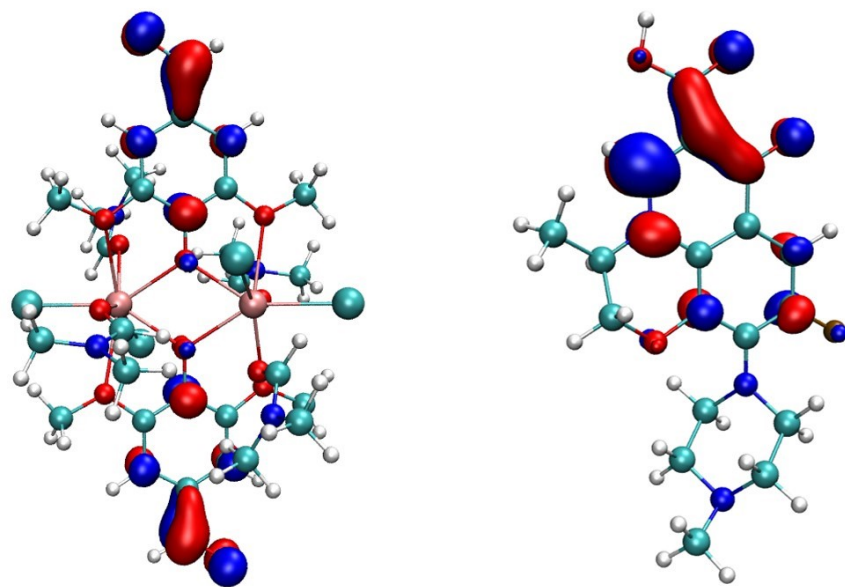


Fig. S13 LUMO electron densities of the ligand in **1** (left) and the free OFX (right) calculated by DFT (Gaussian16 package).

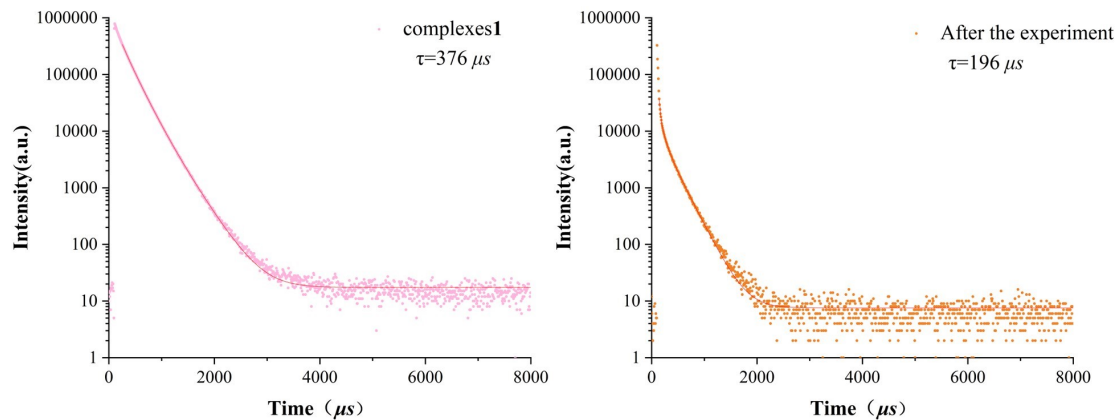


Fig. S14 Fluorescence lifetime spectrum of complex **1** and the fluorescence lifetime of the filter powders following OFX was examined.

The analysis of frontier molecular orbitals

The crystal structure of complex **1** was evaluated using Gaussian16. Single-point energy calculations were performed at the PBE0/6-31G** level for C, H, O, N and Cl atoms, and at the PBE0/MWB54 level for Tb. All atoms in the interfering species were also subjected to single-point energy calculations at the PBE0/6-31G** level. Dispersion corrections were applied using Becke-Johnson (BJ) damping (keyword: em=gd3bj).^[1]

References

1. M. J. Frisch, G. W. Trucks, H. B. Schlegel, G. E. Scuseria, M. A. Robb, J. R. Cheeseman, G. Scalmani, V. Barone, G. A. Petersson, H. Nakatsuji, X. Li, M. Caricato, A. V. Marenich, J. Bloino, B. G. Janesko, R. Gomperts, B. Mennucci, H. P. Hratchian, J. V. Ortiz, A. F. Izmaylov, J. L. Sonnenberg, D. Williams-Young, F. Ding, F. Lipparini, F. Egidi, J. Goings, B. Peng, A. Petrone, T. Henderson, D. Ranasinghe, V. G. Zakrzewski, J. Gao, N. Rega, G. Zheng, W. Liang, M. Hada, M. Ehara, K. Toyota, R. Fukuda, J. Hasegawa, M. Ishida, T. Nakajima, Y. Honda, O. Kitao, H. Nakai, T. Vreven, K. Throssell, J. A. Montgomery Jr., J. E. Peralta, F. Ogliaro, M. J. Bearpark, J. J. Heyd, E. N. Brothers, K. N. Kudin, V. N. Staroverov, T. A. Keith, R. Kobayashi, J. Normand, K. Raghavachari, A. P. Rendell, J. C. Burant, S. S. Iyengar, J. Tomasi, M. Cossi, J. M. Millam, M. Klene, C. Adamo, R. Cammi, J. W. Ochterski, R. L. Martin, K. Morokuma, O. Farkas, J. B. Foresman and D. J. Fox, *Journal*, 2016.